Available online at www.sciencedirect.com
SCIENCE DIRECT®
ELSEVIER
Polymer Testing 23 (2004) 175–185
POLYMER TESTING
www.elsevier.com/locate/polytest

Material Behaviour

Non-isothermal melt crystallization kinetics for poly(trimethylene terephthalate)/poly(butylene terephthalate) blends

Pitt Supaphol *, Nujalee Dangseeyun, Phornphon Srimoaon

The Petroleum and Petrochemical College, Chulalongkorn University, Soi Chula 12, Phyathai Road, Pathumwan, Bangkok 10330, Thailand

Received 22 April 2003; accepted 28 June 2003

Abstract

Various macrokinetic models, namely the Avrami, Ozawa, and Ziabicki models, were applied to describe the non-isothermal melt crystallization process of poly(trimethylene terephthalate) (PTT), poly(butylene terephthalate) (PBT), and their blends. Both the Avrami and the Ozawa models were found to describe the experimental data fairly well. Among the blend compositions studied, Ziabicki's kinetic crystallizability parameter was found to decrease with increasing PTT content. The effective energy barrier for non-isothermal crystallization process of these blends, analyzed based on the differential iso-conversional method of Friedman, was found to be an increasing function of the relative degree of melt conversion. Within the relative degree of melt conversion range of less than ca. 0.5, the effective energy barrier was found to increase with increasing PTT content.

Keywords: Polymer blend; Poly(trimethylene terephthalate); Poly(butylene terephthalate); Non-isothermal crystallization kinetics

1. Introduction

A successful synthesis of poly(trimethylene terephthalate) (PTT) was first reported in 1941 by Whinfield and Dickson [1], but it was not commercially available then due to the high production cost of one of its reactants, 1,3-propanediol. Thanks to a breakthrough in the production of 1,3-propanediol at a much cheaper cost, PTT has been produced by Shell Chemicals under the trade name Corterra™. PTT has properties intermediate between those of poly(ethylene terephthalate) (PET) and poly(butylene terephthalate) (PBT), with an unusual combination of the outstanding properties of PET and processing characteristics of PBT.

Polymer blending is a straightforward, versatile, and relatively inexpensive method for creating a new polymeric material, which has desirable properties of all the constituent components, without the need to synthesize a totally new material which has proven to be too expensive for certain applications. Due to the similarity in the chemical structure of these three linear aromatic polyesters, studies related to blends of a given pair of these polymers should be of high interest. Studies on various aspects for blends of PET and PBT [2–5] and of PET and PTT (or modified PTT) [6–8] are available in the open literature, while those for blends of PTT and PBT, to the best of our knowledge, have not yet been available.

Studies related to the kinetics of polymer crystallization are of great importance in polymer processing, due to the fact that the resulting physical properties are strongly dependent on the morphology formed and the extent of crystallization occurring during processing. It

* Corresponding author. Tel.: +66-2218-4134; fax: +66-2215-4459.
E-mail address: pitt.s@chula.ac.th (P. Supaphol).

0142-9418/$ - see front matter © 2003 Elsevier Ltd. All rights reserved.
doi:10.1016/S0142-9418(03)00078-3

is therefore very important to understand the processing–structure–property interrelationships of the studied materials. To the best of our knowledge, studies related to crystallization behavior for a given pair of the three linear aromatic polyesters are very limited. Relevant reports have been available for blends of PET and PBT [3] and of PET and modified PTT [7,8].

In the present contribution, the non-isothermal crystallization kinetics for blends of PTT and PBT, as compared to those for the pure components (i.e., PTT and PBT), was investigated using differential scanning calorimetry (DSC). The experimental data were analyzed based on the Avrami, Ozawa, and Ziabicki macrokinetic models. The effective energy barrier for the non-isothermal crystallization process for these blends was estimated based on the differential iso-conversional method of Friedman.

2. Theoretical background

The most common approach used to describe the overall isothermal crystallization kinetics is the Avrami model [9–11], in which the relative crystallinity function of time $\theta(t)$ can be expressed as

$$\theta(t) = 1-\exp[-(K_a t)^{n_a}] \in [0,1], \tag{1}$$

where K_a and n_a are the Avrami crystallization rate constant and the Avrami exponent, respectively. Usually, the Avrami rate constant K_a is written in the form of the composite Avrami rate constant k_a (i.e. $k_a = K_a^n$). Since the units of k_a are a function of n_a, use of K_a should be preferable. It should be noted that both K_a and n_a are constants specific to a given crystalline morphology and type of nucleation for a particular crystallization condition [12] and that based on the original assumptions of the theory, the value of the Avrami exponent n_a should be an integer ranging from 1 to 4.

In the study of non-isothermal crystallization using DSC, the energy released during the crystallization process appears to be a function of temperature rather than time as in the case of isothermal crystallization. As a result, the relative crystallinity as a function of temperature $\theta(T)$ can be formulated as

$$\theta(T) = \frac{\int_{T_o}^{T} (dH_c/dT)dT}{\Delta H_c}, \tag{2}$$

where T_o and T represent the onset and an arbitrary temperature, respectively, dH_c is the enthalpy of crystallization released during an infinitesimal temperature range dT, and ΔH_c is the overall enthalpy of crystallization for a specific cooling condition.

To use Eq. (1) for the analysis of non-isothermal crystallization data obtained by DSC, it must be assumed that the sample experiences the same thermal history as designated by the DSC furnace. This may be realized only when the thermal lag between the sample and the furnace is kept minimal. If this assumption is valid, the relation between the crystallization time t and the sample temperature T can be formulated as

$$t = \frac{T_o - T}{\phi}, \tag{3}$$

where ϕ is the cooling rate. According to Eq. (3), the horizontal temperature axis observed in a DSC thermogram for the non-isothermal crystallization data can readily be transformed into the time scale.

Based on the mathematical derivation of Evans [13], Ozawa [14] extended the Avrami theory [9–11] to be able to describe the non-isothermal crystallization data without the need of x-scale transformation. Mathematically, the relative crystallinity function of temperature $\theta(T)$ can be represented as a function of cooling rate as

$$\theta(T) = 1-\exp\left(-\frac{k_o}{\phi^{n_o}}\right) \in [0,1], \tag{4}$$

where k_o is the Ozawa crystallization rate function, and n_o is the Ozawa exponent. It should be noted that the Ozawa kinetic parameters (i.e., k_o and n_o) holds similar physical meanings to those of the Avrami ones.

Instead of describing the crystallization process with complicated mathematical models, Ziabicki [15–17] proposed that the kinetics of polymeric phase transformation can be described by a first-order kinetic equation of the form:

$$\frac{d\theta(t)}{dt} = K_z(T)[1-\theta(t)], \tag{5}$$

where $K_z(T)$ is a temperature-dependent crystallization rate function. In the case of non-isothermal crystallization, both $\theta(t)$ and $K_z(T)$ functions vary and are dependent on the cooling rate used.

For a given cooling condition, Ziabicki [15–17] showed that the crystallization rate function $K_z(T)$ can be described by a Gaussian function of the following form:

$$K_z(T) = K_{z,max}\exp\left[-4\ln 2\frac{(T_c - T_{max})^2}{D^2}\right], \tag{6}$$

where T_{max} is the temperature at which the crystallization rate is maximum, $K_{z,max}$ is the crystallization rate at T_{max}, and D is the half-width of the crystallization rate-temperature function. With use of the isokinetic approximation, integration of Eq. (6) over the whole crystallizable range of temperatures ($T_g < T < T_m^o$), for a given cooling condition, leads to an important characteristic value describing the crystallization ability of a semi-

crystalline polymer, namely, the kinetic crystallizability G_z:

$$G_z = \int_{T_g}^{T_m^o} K_z(T)\mathrm{d}T \approx 1.064 K_{z,\max} D. \quad (7)$$

In the case of non-isothermal crystallization studies using DSC where cooling rate is a variable, Eq. (7) can be applied when the crystallization rate function $K_z(T)$ is replaced with a derivative function of the relative crystallinity function of temperature $(\mathrm{d}\theta/\mathrm{d}T)_\phi$ specific for each cooling rate studied (i.e., crystallization rate function at different cooling rates). Therefore, Eq. (7) is replaced by

$$G_{z,\phi} = \int_{T_g}^{T_m^o} (\mathrm{d}\theta/\mathrm{d}T)_\phi \mathrm{d}T \approx 1.064 (\mathrm{d}\theta/\mathrm{d}T)_{\phi,\max} D_\phi, \quad (8)$$

where $(\mathrm{d}\theta/\mathrm{d}T)_{\phi,\max}$ and D_ϕ are the maximum crystallization rate and the half-width of the derivative relative crystallinity as a function of temperature $(\mathrm{d}\theta/\mathrm{d}T)_\phi$. According to Eq. (5), $G_{z,\phi}$ is the kinetic crystallizability at an arbitrary cooling rate ϕ. The kinetic crystallizability at unit cooling rate G_z can therefore be obtained by normalizing $G_{z,\phi}$ with ϕ (i.e., $G_z = G_{z,\phi}/\phi$). It should be noted that this procedure was first realized by Jeziorny [18].

While offering a simple way of evaluating corresponding kinetic parameters specific to each model, the Avrami, Ozawa, and Ziabicki analyses do not suggest a means for evaluating the effective energy barrier for non-isothermal crystallization process ΔE. In light of this, various mathematical procedures [19–21] were proposed for evaluating the ΔE value. The main objective of these methods is to define a finite relationship between the peak temperature T_p obtained for a given condensed phase reaction and the heating rate ϕ used. A major concern for use of these procedures in obtaining the kinetic information for non-isothermal crystallization process which occurs on cooling has recently been raised [22], since the original mathematic expression for these procedures does not permit substitution of negative heating rates ϕ (i.e., cooling rates). However, this problem has largely been wrongly avoided by dropping off the minus sign in the negative heating rates [23].

For a process that occurs on cooling, such as non-isothermal crystallization of polymer melts, reliable values of the effective energy barrier can be obtained, for example, by the differential iso-conversional method of Friedman [24] or by the integral iso-conversional method of Vyazovkin [25,26]. In this work, the Friedman method will be used, mainly due to the reliability and simplicity of the method [22,26]. The Friedman equation is expressed as

$$\ln(\dot{\theta}_\theta(t)) = A - \frac{\Delta E_\theta}{RT}, \quad (9)$$

where $\dot{\theta}_\theta(t)$ is the instantaneous crystallization rate as a function of time at a given conversion θ, A is an arbitrary pre-exponential parameter, and ΔE_θ is the effective energy barrier of the process at a given conversion θ. By plotting the instantaneous crystallization rate data measured from non-isothermal experiments conducted at various cooling rates against the corresponding inversed temperature for a given conversion θ, the effective energy barrier for non-isothermal crystallization process can be determined.

3. Experimental details

3.1. Materials

Poly(trimethylene terephthalate) (PTT) was supplied in pellet form by Shell Chemicals (USA) (Corterra CP509201). The weight- and number-average molecular weights of this resin were determined to be ca. 78,100 and 34,700 Da, respectively. Poly(butylene terephthalate) (PBT) was supplied in pellet form by LG Chem (Korea) (LUPOX GP-2000). The weight- and number-average molecular weights of this resin were determined to be ca. 71,500 and 36,300 Da, respectively. Molecular weight characterization for these resins was carried out by Dr. Hoe H. Chuah and his co-workers of Shell Chemicals (USA) based on size-exclusion chromatography (SEC).

3.2. Sample preparation

PTT and PBT resins were dried in a vacuum oven at 140 °C for 5 h and then were premixed in a dry mixer to prepare PTT/PBT blends at three compositional w/w ratios of 25/75, 50/50, and 75/25, respectively. For simplicity, these blends are hereafter denoted as 25PTT/75PBT, 50PTT/50PBT, and 75PTT/25PBT, respectively. The dry-mixed blends were melt-mixed in a self-wiping, co-rotating twin-screw extruder (Collin, ZX-25) using a die temperature of 280 °C and a screw speed of 70 rpm, and then cut into pellet form by a pelletizer (Planetrol, 075D2). Films of approximately 200 μm in thickness for neat resins and their blends were prepared by a compression press (Wabash, V50H). The set temperature and the applied pressure were 260 °C and 15 ton-force, respectively. After 5 min holding time in the press, the films were taken out and allowed to cool, under the ambient condition, down to room temperature.

3.3. Differential scanning calorimetry measurements

A differential scanning calorimeter (DSC) (Perkin–Elmer, DSC-7), equipped with an intracooling unit capable of maintaining the chamber temperature at -10 ± 0.5 °C, was used to record non-isothermal melt crystallization exotherms and subsequent melting endo-

therms for PTT, PBT, and their blends. Calibration for the temperature scale was carried out using a pure indium standard (T_m^o = 156.6 °C and ΔH_f^o = 28.5 J g^{-1}) on every other run to ensure accuracy and reliability of the data obtained. To minimize thermal lag between the polymer sample and the DSC furnace, each sample holder was loaded with a disc-shape sample weighing around 8.0 ± 0.5 mg which was cut from the as-prepared films. It is assumed that thermal lags were the same for both heating and cooling scans. To prevent extensive thermal degradation, each sample was used only once and all the runs were carried out under a nitrogen atmosphere.

The experiment started with heating each sample from 40 °C at a heating rate of 80 °C·min^{-1} to a fixed melt-annealing temperature T_f of 280 °C for a melt-annealing period t_h of 5 min in order to ensure complete melting. After this period, each sample was cooled at the desired cooling rate ϕ, ranging from 5 to 50 °C min^{-1}, to 30 °C. The non-isothermal melt crystallization exotherms were recorded and analyzed according to the models aforementioned.

4. Results and discussion

4.1. Non-isothermal melt crystallization behavior

The typical non-isothermal melt crystallization exotherms for 50PTT/50PBT for indicated cooling rates are shown, as examples, in Fig. 1. The single crystallization exotherm observed for each cooling rate suggests that both PTT and PBT crystallized simultaneously during cooling. Similar behavior was also observed for blends of other compositions studied. With increasing cooling rate, the exothermic trace became wider and shifted towards lower temperatures. The observation is general for both pure and blend samples studied. Table 1 summarizes characteristic data for non-isothermal melt crystallization of all of the samples studied. For each resin, the temperature at 1% relative crystallinity $T_{0.01}$, the temperature at the maximum crystallization rate (i.e., the peak temperature) T_p, and the temperature at 99% relative crystallinity $T_{0.99}$ were all shifted towards lower temperatures with increasing cooling rate. The values of $T_{0.01}$ and $T_{0.99}$ will be hereafter used to represent the beginning and the ending of the crystallization process. The fact that all of the $T_{0.01}$, T_p, and $T_{0.99}$ values decreased with increasing cooling rate implies that the higher the cooling rate, the later the crystallization process began and ended (based on the temperature domain).

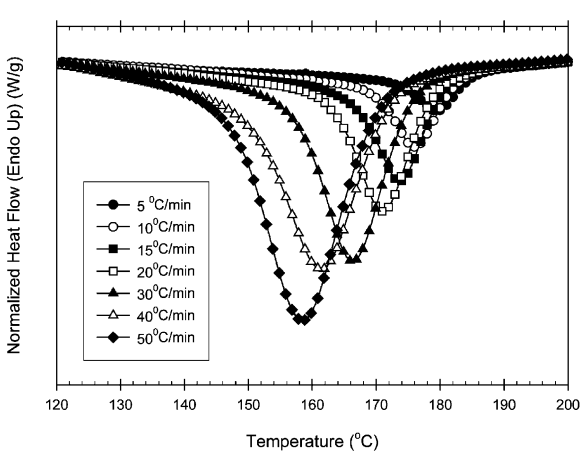

Fig. 1. Non-isothermal melt crystallization exotherms for 50PTT/50PBT blend for seven different cooling rates, ranging from 5 to 50 °C min^{-1}.

For a given cooling rate, all of the $T_{0.01}$, T_p, and $T_{0.99}$ values for PBT were consistently higher and those for PTT, suggesting that PBT was more readily crystallized than PTT. The $T_{0.01}$, T_p, and $T_{0.99}$ values for 25PTT/75PBT blend were consistently lower than those for pure PBT, but higher than those for pure PET, for all of the cooling rates studied. For the 50PTT/50PBT blend, the $T_{0.01}$, T_p, and $T_{0.99}$ values obtained for cooling rates of 5 and 10 °C min^{-1} were found to be lower than those for pure PTT, while those obtained for higher cooling rates were found to be higher than those for pure PTT. For 75PTT/25PBT blend, the values obtained for cooling rates of 5–30 °C min^{-1} were found to be lower than those for pure PTT, while those obtained for higher cooling rates were found to be higher than those for pure PTT. These results suggest that the presence of the less crystallizable PTT molecules in the blends reduced the crystallizability of the blends and that the mechanism for non-isothermal melt crystallization depended very much on the cooling rate used.

4.2. Non-isothermal melt crystallization kinetics

To further obtain relevant non-isothermal melt crystallization kinetic information, the experimental data such as those shown in Fig. 1 need to be presented either as the relative crystallinity function of temperature $\theta(T)$ or of time $\theta(t)$, depending on the macrokinetic model used. The conversion from the raw data into the $\theta(T)$ function can be carried out using Eq. (2). Once the $\theta(T)$ function is obtained, conversion into the $\theta(t)$ function can be carried out by transforming the temperature scale into the time scale using Eq. (3). Figs. 2 and 3 illustrate, for example, the $\theta(T)$ and the $\theta(t)$ functions for the 50PTT/50PBT blend. These functions were converted from the raw data shown in Fig. 1 using Eqs. (2) and (3), respectively.

An important parameter which can be taken from the $\theta(t)$ function is the half-time of crystallization $t_{0.5}$, which is the time interval from the onset of the crystallization

Table 1
Characteristic data of non-isothermal melt crystallization exotherms for PBT, PTT, and their blends

ϕ (°C min^{-1})	PBT			25PTT/75PBT			50PTT/50PBT			75PTT/25PBT			PTT		
	$T_{0.01}$ (°C)	T_p (°C)	$T_{0.99}$ (°C)	$T_{0.01}$ (°C)	T_p (°C)	$T_{0.99}$ (°C)	$T_{0.01}$ (°C)	T_p (°C)	$T_{0.99}$ (°C)	$T_{0.01}$ (°C)	T_p (°C)	$T_{0.99}$ (°C)	$T_{0.01}$ (°C)	T_p (°C)	$T_{0.99}$ (°C)
5	206.7	196.9	189.2	199.7	190.1	181.6	187.0	179.7	171.2	186.8	178.2	164.6	192.7	185.8	179.2
10	204.5	192.1	184.8	196.1	187.0	180.6	185.8	176.1	166.7	184.7	175.3	158.2	188.2	178.6	170.7
15	201.8	187.2	177.6	193.7	183.7	175.5	184.5	173.7	159.6	180.8	172.0	152.3	184.2	173.5	163.0
20	198.6	186.9	172.9	193.7	180.9	168.7	182.9	170.9	155.5	178.9	168.9	146.7	181.6	170.3	160.2
30	196.6	181.4	169.1	189.6	176.9	164.0	179.0	166.4	146.3	174.8	164.4	141.7	177.6	163.9	148.4
40	193.6	176.5	164.3	188.1	173.2	155.9	174.8	161.2	143.4	177.6	161.2	132.3	173.9	158.5	139.1
50	191.5	174.0	159.1	185.3	169.0	147.4	172.7	158.2	142.5	168.2	157.3	128.2	169.7	153.2	130.4

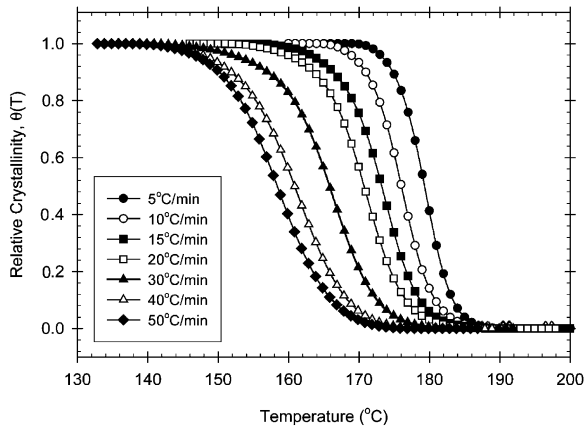

Fig. 2. Relative crystallinity functions of temperature for 50PTT/50PBT blend for seven different cooling rates, ranging from 5 to 50 °C min^{-1}.

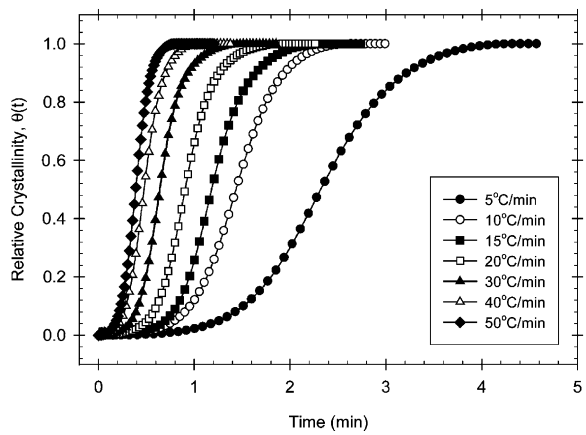

Fig. 3. Relative crystallinity functions of time for 50PTT/50PBT blend for seven different cooling rates, ranging from 5 to 50 °C min^{-1}.

to the time at 50% completion. According to Fig. 3, the $t_{0.5}$ value decreased with increasing cooling rate, indicating that this particular blend crystallized faster when the cooling rate was increased. This observation is generally true for all of the sample types studied. The inverse value of $t_{0.5}$ (i.e., $t_{0.5}^{-1}$) signifies the bulk crystallization rate. Table 2 summarizes the $t_{0.5}^{-1}$ values for PTT, PBT, and blend samples studied. Clearly, for a given sample type, the $t_{0.5}^{-1}$ value was found to increase with increasing cooling rate. Comparison of the $t_{0.5}^{-1}$ values for all of the sample types suggests that the 50PTT/50PBT blend crystallized the fastest, while PTT crystallized the slowest.

In order to quantitatively compare non-isothermal crystallization rates obtained for different polymer systems, two approaches can be used: (1) the crystallization rate coefficient (CRC) [27] and (2) the crystallization rate parameter (CRP) [28]. The CRC can be determined

Table 2
Non-isothermal melt crystallization kinetics for PBT, PTT, and their blends based on Avrami analysis

ϕ (°C min^{-1})	PBT				25PTT/75PBT				50PTT/50PBT				75PTT/25PBT				PTT			
	n_a	K_a (min^{-1})	r^2	$t_{0.5}^{-1}$ (min^{-1})	n_a	K_a (min^{-1})	r^2	$t_{0.5}^{-1}$ (min^{-1})	n_a	K_a (min^{-1})	r^2	$t_{0.5}^{-1}$ (min^{-1})	n_a	K_a (min^{-1})	r^2	$t_{0.5}^{-1}$ (min^{-1})	n_a	K_a (min^{-1})	r^2	$t_{0.5}^{-1}$ (min^{-1})
5	3.98	0.37	0.9997	0.40	4.21	0.37	0.9993	0.40	4.07	0.39	0.9995	0.43	3.39	0.32	0.9988	0.36	3.78	0.42	0.9997	0.34
10	6.17	0.45	1.0000	0.48	5.09	0.72	0.9998	0.78	4.38	0.64	0.9996	0.70	4.13	0.54	0.9952	0.61	4.05	0.64	0.9991	0.55
15	4.56	0.73	0.9998	0.79	5.33	0.91	0.9997	0.97	4.45	0.77	0.9987	0.85	3.09	0.80	0.9952	0.94	3.92	0.86	0.9999	0.74
20	3.97	1.03	0.9983	1.13	4.97	0.98	0.9620	1.06	4.25	1.00	0.9990	1.11	3.68	1.01	0.9953	1.15	3.86	1.17	0.9999	1.02
30	4.71	1.18	0.9999	1.27	5.75	1.27	0.9994	1.36	3.90	1.40	0.9985	1.56	3.66	1.24	0.9964	1.42	3.62	1.35	0.9998	1.11
40	3.73	1.73	0.9998	1.89	5.30	1.44	0.9991	1.55	3.43	1.87	0.9994	2.10	3.74	1.36	0.9972	1.54	3.20	1.26	1.0000	1.21
50	3.62	2.11	0.9998	2.31	4.34	1.80	0.9986	1.99	3.60	2.31	0.9998	2.57	2.69	2.12	0.9972	2.53	3.73	1.68	0.9998	1.65

from the slope of a line drawn through a plot of the cooling rate against the peak temperature T_p. According to Khanna [27], the CRC parameter can be used as a guide for ranking different polymer systems on a single scale of crystallization rates. The higher the CRC value, the faster the crystallization rate for the polymer system of interest. The CRP can be determined from the slope of a line drawn through a plot of the reciprocal half-time $t_{0.5}^{-1}$ versus the cooling rate. Since the faster the crystallization rate of a polymer system, the higher the slope is, the CRP parameter can be used to rank the relative crystallization rate for different polymer systems.

Fig. 4a and b show plots of the cooling rate as a function of T_p and plots of $t_{0.5}^{-1}$ as a function of the cooling rate. From the slopes of the straight lines drawn through the bulk of the data, values of the CRC and CRP parameters can be determined. These values are summarized in Table 3. The CRC values for PBT and PTT were ca. 1.96 and 1.42 min^{-1}, respectively, indicating that PBT was more crystallizable than PTT. The CRP values for PBT and PTT were ca. 0.043 and 0.026 K^{-1}, respect-

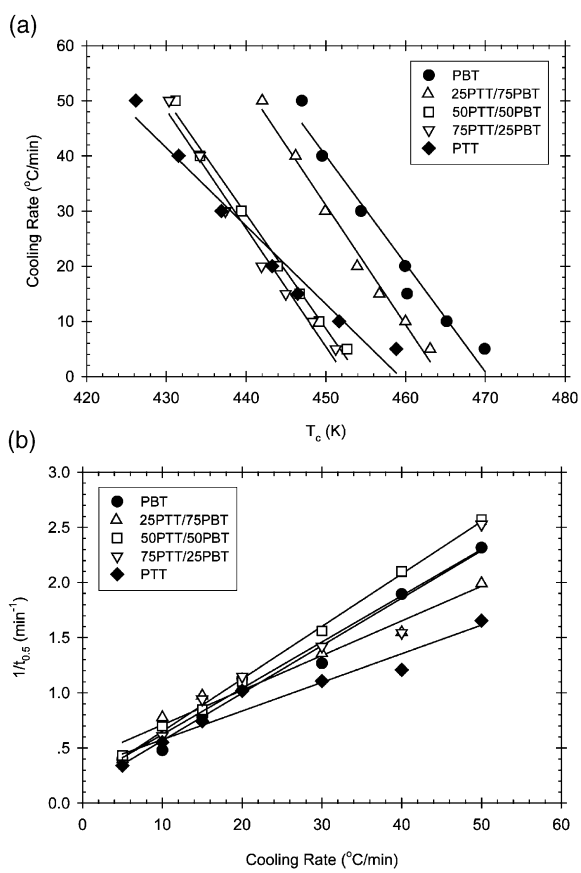

Fig. 4. (a) Plots of cooling rate as a function of the temperature at the maximum crystallization rate and (b) plots of reciprocal half-time of crystallization as a function of the cooling rate for PTT, PBT, and their blends.

Table 3
CRC and CRP values for PBT, PTT, and their blends

	PBT	25PTT/75PBT	50PTT/50PBT	75PTT/25PBT	PTT
CRC (min^{-1})	1.96	2.17	2.08	2.14	1.42
CRP (K^{-1})	0.043	0.032	0.048	0.042	0.026

ively, also suggesting that PBT was more crystallizable than PTT. Based on the CRC values obtained, the crystallization ability of all of the sample types studied followed the order: 25PTT/75PBT > 75PTT/25PBT > 50PTT/50PBT > PBT > PTT, while, based on the CRP values obtained, it was in the order: 50PTT/50PBT > PBT≈75PTT/25PBT > 25PTT/75PBT > PTT. Obviously, both CRC and CRP approaches were not decisive in the ranking of the crystallization ability for PTT, PBT, and their blends.

4.2.1. Avrami analysis

Data analysis based on the Avrami macrokinetic model was carried out by directly fitting the experimental $\theta(t)$ data, such as those shown in Fig. 3, to Eq. (1), using a non-linear multi-variable regression program. Only the relative crystallinity data in the range of 10–80% were used in the fitting. Table 2 summarizes values of the Avrami kinetic parameters (i.e., n_a and K_a) as well as the values of the correlation parameter r^2 for all of the samples studied.

The n_a values for PTT and PBT were found to be in the range of ca. 3.2 to 4.1 and from ca. 3.6 to 6.2, respectively. Wang et al. [24] reported the n_a values for a PTT resin having the number-average molecular weight of ca. 23,000 Da in the range of ca. 3.3 to 4.0, over the cooling rate range of 0.63 to 20 °C min^{-1}, which are in excellent agreement with our results. For PTT/PBT blends, the n_a values were found to range from ca. 4.2 to 5.8 for 25PTT/75PBT blend, from ca. 3.4 to 4.5 for 50PTT/50PBT blend, and from ca. 2.7 to 4.1 for 75PTT/25PBT blend, with a tendency for the n_a value to decrease with increasing PTT content at a given cooling rate.

Similar to the case of $t_{0.5}^{-1}$, values of K_a were found to be strongly dependent on the cooling rate. For a given sample type, K_a was found to increase with increasing cooling rate, suggesting that each polymer system crystallized faster when the cooling rate was increased. Similarity between the K_a and $t_{0.5}^{-1}$ values is not surprising, since these two bulk CRPs are related (i.e., $K_a = (\ln 2)^{1/n} t_{0.5}^{-1}$). Comparatively, PTT was found to crystallize a bit faster than PBT when the cooling rates were lower than ca. 30 °C·min^{-1}, while it crystallized a bit slower than PBT at the cooling rates greater than ca. 30 °C·min^{-1}. This is contradictory to the observation based on the $t_{0.5}^{-1}$ values, in which PTT was found to crystallize slower than PBT at any given cooling rate. The slight discrepancy may be a result of the use of the relative crystallinity data in the range of 10–80% for the fitting and the selection of the baseline during the conversion of the raw crystallization exotherm data into the relative crystallinity function of temperature (or time). Based on the K_a values summarized in Table 2, PTT was the fastest to crystallize when the cooling rates were lower than ca. 20 °C·min^{-1}, while 50PTT/50PBT blend crystallized the fastest for cooling rates greater than ca. 20 °C·min^{-1}.

4.2.2. Ozawa analysis

The Ozawa kinetic parameters (i.e., k_o and n_o) can be extracted by drawing a least-squared line to the double-logarithmic plot of $\ln[-\ln(1-\theta(T))]$ versus $\ln(\phi)$ for a fixed temperature, where k_o is taken as the anti-logarithmic value of the y-intercept and n_o is simply the negative value of the slope. Fig. 5 shows such a plot for 25PTT/75PBT blend, as examples, while values of the Ozawa kinetic parameters (i.e., n_o and k_o) as well as values of the r^2 parameter for all of the samples studied are summarized in Table 4.

The values of r^2 listed in Table 4 suggest that the Ozawa model provided a satisfactory description to the non-isothermal melt crystallization for these polymer systems. In all cases, values of n_o were found to range from ca. 0.3 to 4.5. More specifically, n_o ranged from ca. 1.9 to 2.7 for PBT within the temperature range of

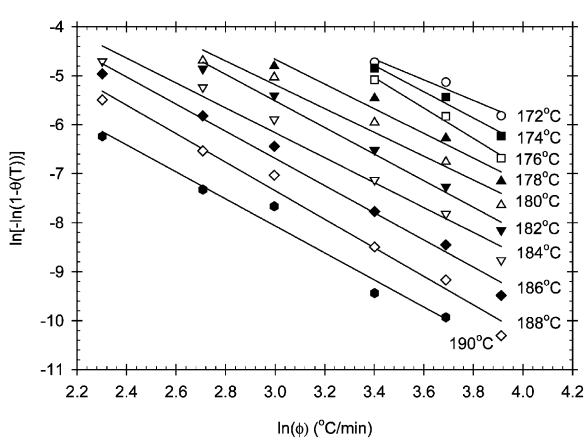

Fig. 5. Typical Ozawa analysis based on the non-isothermal crystallization data of 25PTT/75PBT blend.

Table 4
Non-isothermal melt crystallization kinetics for PBT, PTT, and their blends based on Ozawa analysis

PBT				25PTT/75PBT			50PTT/50PBT				75PTT/25PBT				PTT			
Temp (°C)	n_o	k_o (°C $min^{-1})^{n_o}$	r^2	Temp (°C)	n_o	k_o (°C $min^{-1})^{n_o}$	r^2	Temp (°C)	n_o	k_o (°C $min^{-1})^{n_o}$	r^2	Temp (°C)	n_o	k_o (°C $min^{-1})^{n_o}$	r^2	Temp (°C)	n_o	k_o (°C $min^{-1})^{n_o}$	r^2
180	2.06	1.11×10^3	0.9852	172	2.10	1.20×10^1	0.9531	160	1.46	1.19	0.9987	154	0.30	2.31×10^{-2}	0.9795	160	2.65	1.14×10^4	0.9779
182	2.20	1.24×10^3	0.9949	174	2.68	7.62×10^1	0.9761	162	1.98	6.22	1.0000	156	0.39	2.98×10^{-2}	0.9773	164	3.03	1.80×10^4	0.9724
184	2.24	9.36×10^2	0.9935	176	3.11	2.53×10^2	0.9871	164	2.51	3.21×10^1	0.9987	158	0.53	4.49×10^{-2}	0.9776	166	3.24	2.41×10^4	0.9769
186	2.03	2.96×10^2	0.9736	178	2.52	1.80×10^1	0.9606	166	3.00	1.29×10^2	0.9961	160	0.75	8.36×10^{-2}	0.9842	168	3.47	3.25×10^4	0.9827
188	2.14	2.51×10^2	0.9730	180	2.43	8.28	0.9698	168	2.78	3.41×10^1	0.9774	162	0.83	9.04×10^{-2}	0.9451	170	3.83	5.05×10^4	0.9729
190	1.94	1.04×10^2	0.9898	182	2.71	1.43×10^1	0.9892	170	3.28	1.15×10^2	0.9861	164	1.15	2.04×10^{-1}	0.9571	172	4.13	7.46×10^4	0.9737
192	2.12	9.64×10^1	0.9959	184	2.55	4.37	0.9765	172	3.73	3.11×10^2	0.9896	166	1.19	1.71×10^{-1}	0.9139	174	4.54	1.34×10^5	0.9700
194	2.28	7.94×10^1	0.9987	186	2.78	5.14	0.9867	174	3.74	1.44×10^2	0.9770	168	1.55	3.82×10^{-1}	0.9318	176	4.33	4.26×10^4	0.9908
196	2.46	6.24×10^1	0.9979	188	2.92	4.06	0.9846	176	4.43	6.04×10^2	0.9599	170	1.93	8.44×10^{-1}	0.9425	178	3.72	3.57×10^3	0.9872
198	2.69	5.08×10^1	0.9909	190	2.37	3.56×10^{-1}	0.9669	–	–	–	–	172	2.30	1.56	0.9355	180	4.03	3.60×10^3	0.9852

180 to 198 °C and from ca. 2.7 to 4.5 for PTT within the temperature range of 160 to 180 °C. In the blends, n_o was found to range from ca. 2.1 to 3.1 for 25PTT/75PBT blend within the temperature range of 172 to 190 °C, from ca. 1.5 to 4.4 for 50PTT/50PBT blend within the temperature range of 160 to 176 °C, and from ca. 0.3 to 2.3 for 75PTT/25PBT blend within the temperature range of 154 to 172 °C, respectively. In the case of PTT, the values of n_o obtained here were greater than those reported by Wang et al. [29], who found that n_o values for the PTT resin having the number-average molecular weight of ca. 23,000 Da were in the range of 1.7 to 3.1 within the temperature range of 160 to 192 °C. For all of the sample types studied, k_o was found to decrease with increasing temperature (within the temperature range investigated), suggesting that these polymer systems crystallized slower when the temperature increased.

4.2.3. Ziabicki's kinetic crystallizability analysis

Analysis according to the modified first order Ziabicki's kinetic equation (i.e., Eq. (8)) can be carried out by differentiating the $\theta(T)$ function, such as those shown in Fig. 2, in order to obtain the derivative relative crystallinity as a function of temperature $(d\theta/dT)_\phi$. Once the $(d\theta/dT)_\phi$ function is obtained, various kinetic parameters (i.e., the maximum crystallization rate $(d\theta/dT)_{\phi,max}$ and the half-width of the $(d\theta/dT)_\phi$ function D_ϕ) can then be obtained and, finally, the cooling rate-dependent kinetic crystallizability $G_{z,\phi}$ can be calculated using Eq. (8).

Table 5 summarizes the values of $T_{\phi,max}$ (i.e., the temperature at the maximum crystallization rate as determined from the $(d\theta/dT)_\phi$ functions), $(d\theta/dT)_{\phi,max}$, D_ϕ and G_z for all of samples studied. It should be noted that the $T_{\phi,max}$ values listed in Table 5 and T_p (i.e., the temperature at the maximum crystallization rate as determined from the raw non-isothermal melt crystallization exotherms) listed in Table 1 are almost identical for all of the samples studied. For a given sample type, the $T_{\phi,max}$ value was found to decrease, while both $(d\theta/dT)_{\phi,max}$ and D_ϕ values were all found to increase, with increasing cooling rate. Based on these values, the resulting $G_{z,\phi}$ value (not listed) was therefore an increasing function of the cooling rate. By normalizing the effect of the cooling rate from the resulting $G_{z,\phi}$ value, the value of the kinetic crystallizability at unit cooling rate G_z can therefore be determined and the results summarized in Table 5 confirmed that the normalized G_z values for each sample type for different cooling rate were very comparable.

Since the physical meaning of the G_z parameter is to characterize the ability of a semi-crystalline polymer to crystallize when it is cooled from its equilibrium melting temperature to the glass transition temperature at unit cooling rate, the higher the G_z value, the more readily the polymer crystallizes. Based on the average G_z values summarized in Table 5, the crystallization ability for all

Table 5
Non-isothermal melt crystallization kinetics for PBT, PTT, and their blends based on Ziabicki analysis

ϕ (°C min^{-1})	PBT				25PTT/75PBT				50PTT/50PBT				75PTT/25PBT				PTT			
	$T_{\phi,max}$ (°C)	$(d\theta/dT)_{\phi,max}$ (s^{-1})	D_ϕ (°C)	G_z	$T_{\phi,max}$ (°C)	$(d\theta/dT)_{\phi,max}$ (s^{-1})	D_ϕ (°C)	G_z	$T_{\phi,max}$ (°C)	$(d\theta/dT)_{\phi,max}$ (s^{-1})	D_ϕ (°C)	G_z	$T_{\phi,max}$ (°C)	$(d\theta/dT)_{\phi,max}$ (s^{-1})	D_ϕ (°C)	G_z	$T_{\phi,max}$ (°C)	$(d\theta/dT)_{\phi,max}$ (s^{-1})	D_ϕ (°C)	G_z
5	196.9	9.79×10^{-3}	13.10	1.64	190.1	1.14×10^{-2}	12.10	1.76	179.6	1.11×10^{-2}	9.22	1.30	178.3	8.69×10^{-3}	11.01	1.22	185.8	1.05×10^{-2}	9.84	1.31
10	192.1	1.71×10^{-2}	17.44	1.91	187.0	2.47×10^{-2}	12.97	2.05	176.1	1.81×10^{-2}	13.38	1.55	175.5	2.15×10^{-2}	11.48	1.58	178.6	1.91×10^{-2}	11.52	1.41
15	187.2	2.11×10^{-2}	21.69	1.95	183.9	3.48×10^{-2}	12.95	1.92	173.7	2.54×10^{-2}	12.97	1.40	172.2	2.83×10^{-2}	10.94	1.32	173.5	2.23×10^{-2}	19.66	1.86
20	186.9	2.56×10^{-2}	17.80	1.45	181.3	3.87×10^{-2}	15.53	1.92	170.9	3.09×10^{-2}	17.90	1.77	168.9	3.71×10^{-2}	11.90	1.41	170.3	2.99×10^{-2}	18.37	1.75
30	181.4	3.55×10^{-2}	20.65	1.56	176.9	5.23×10^{-2}	16.64	1.85	166.4	4.02×10^{-2}	18.03	1.54	164.4	4.50×10^{-2}	11.70	1.12	163.9	3.26×10^{-2}	20.36	1.41
40	177.2	4.03×10^{-2}	24.00	1.54	173.2	5.39×10^{-2}	18.82	1.62	161.2	4.43×10^{-2}	20.65	1.46	160.5	4.77×10^{-2}	14.03	1.07	158.5	3.67×10^{-2}	24.99	1.46
50	174.0	5.03×10^{-2}	25.67	1.65	169.0	5.86×10^{-2}	21.10	1.58	158.2	5.29×10^{-2}	23.41	1.58	157.3	5.30×10^{-2}	17.42	1.18	152.3	3.63×10^{-2}	28.46	1.32
	Average			1.67	Average			1.81	Average			1.51	Average			1.27	Average			1.50

of the sample types studied followed the following order: 25PTT/75PBT > PBT > 50PTT/50PBT≈PTT > 75PTT/25PBT.

4.2.4. Effective energy barrier for non-isothermal melt crystallization process

Analysis based on the differential iso-conversional method of Friedman [24] can be carried out by first differentiating the $\theta(t)$ function with respect to time to obtain the instantaneous crystallization rate as a function of time $\dot{\theta}(t)$. A plot according to Eq. (9) can then be performed for various values of relative melt conversion (i.e., relative crystallinity) using the data obtained from both $\dot{\theta}(t)$ and $\theta(T)$ functions and the effective energy barrier of the non-isothermal melt crystallization process for a given relative melt conversion θ (i.e., ΔE_θ) can finally be estimated from the slope of the plot (i.e., $\Delta E_\theta = -(\text{slope})(R)$).

Fig. 6 illustrates plots of the effective activation energy ΔE as a function of the relative melt conversion for all of the sample types studied, while the observed ΔE values are summarized in Table 6. For all of the sample types studied, ΔE was generally found to increase with increasing relative melt conversion, suggesting that as the crystallization proceeded it was more difficult for each polymer system to crystallize. As crystallization proceeds, diffusion of the crystallizing molecular segments from the equilibrium melt to the growth front will be retarded by the rejected molecular species. For θ's lower than ca. 0.5, the ΔE values for all of the sample types studied were in the following sequence: PBT < 25PTT/75PBT < 50PTT/50PBT≈75PTT/25PBT < PTT. For θ's greater than ca. 0.5 but lower than ca. 0.9, they were in the order: PBT < 50PTT/50PBT < 25PTT/75PBT < 75PTT/25PBT < PTT. For θ's greater than ca. 0.9, they were in the following order: PBT < 50PTT/50PBT < PTT≈25PTT/75PBT <

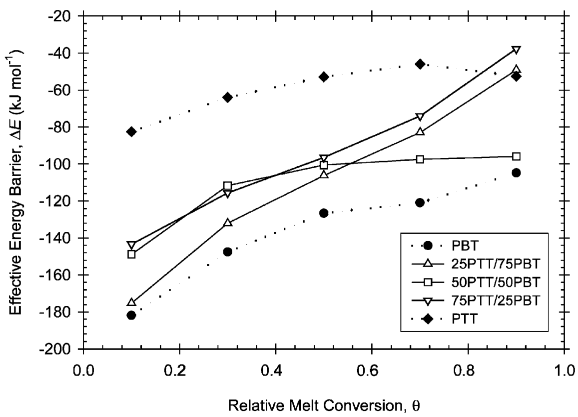

Fig. 6. Plots of the effective energy barrier for non-isothermal melt crystallization of PTT, PBT, and their blends as a function of the relative degree of melt conversion.

Table 6
Effective energy barrier describing the non-isothermal melt crystallization process for PBT, PTT, and their blends based on Friedman method

Sample	Effective energy barrier ΔE (kJ mol^{-1})				
	$\theta = 0.1$	$\theta = 0.3$	$\theta = 0.5$	$\theta = 0.7$	$\theta = 0.9$
PBT	−181.9	−147.7	−126.6	−121.0	−104.9
25PTT/75PBT	−175.2	−132.1	−106.2	−82.9	−49.1
50PTT/50PBT	−148.8	−111.7	−100.5	−97.5	−95.9
75PTT/25PBT	−143.4	−115.7	−96.4	−74.0	−37.7
PTT	−82.6	−64.0	−52.9	−46.0	−52.5

75PTT/25PBT. It should be noted that the lower the ΔE value, the higher the crystallization ability of the polymer system of interest becomes.

5. Conclusions

The non-isothermal melt crystallization exotherms for PTT, PBT, and their blends showed that the temperature at 1% relative crystallinity, the temperature at the maximum crystallization rate, and the temperature at 99% relative crystallinity were all shifted towards lower temperatures with increasing cooling rate. The half-time of crystallization was found to decrease with increasing cooling rate, suggesting that these polymer systems spent shorter time intervals to crystallize when the cooling rate increased. Both the Avrami and Ozawa macrokinetic models provided a satisfactory description of the experimental data.

Based on the values of the reciprocal half-time of crystallization, 50PTT/50PBT blend was found to crystallize the fastest, while PTT crystallized the slowest. Based on the CRC approach, the crystallization ability for PTT, PBT, and their blends was in the following order: 25PTT/75PBT > 75PTT/25PBT > 50PTT/50PBT > PBT > PTT, while, based on the CRP approach, it was in the order: 50PTT/50PBT > PBT≈75PTT/25PBT > 25PTT/75PBT > PTT. The crystallization ability for all of the sample types studied as suggested by the Ziabicki's kinetic crystallizability was in the following sequence: 25PTT/75PBT > PBT > 50PTT/50PBT≈ PTT > 75PTT/25PBT, while, based on the effective energy barrier for non-isothermal melt crystallization process at 'low' values of relative melt conversion (i.e., ca. <0.5), it was in the order: PBT > 25PTT/75PBT > 50PTT/50PBT≈75PTT/25PBT > PTT.

Acknowledgments

The authors wish to thank Dr. Hoe H. Chuah and his co-workers of Shell Chemical Company (USA) Ltd. for supplying of PTT and for their kind assistance on molecular weight measurements on PTT and PBT resins, and Dr. Gi-Dae Choi and Soo-Min Lee of LG Chem (Korea) Ltd. for supplying of PBT. PS acknowledges a grant provided by Chulalongkorn University through the Development Grants for New Faculty/Researchers. Partial support from the Petroleum and Petrochemical Technology Consortium and the Petroleum and Petrochemical College is greatly acknowledged.

References

[1] J.R. Whinfield, J.T. Dickson, Brit Pat 578,079, June 14, 1946.
[2] B. Jacques, J. Devaux, R. Legras, E. Nield, Polymer 38 (1997) 5367.
[3] T.K. Kang, Y. Kim, C.S. Ha, J. Appl. Polym. Sci. 74 (1999) 1797.
[4] S.C.E. Backsona, R.W. Richards, S.M. King, Polymer 40 (1999) 4205.
[5] K.J. Song, J.L. White, Polym. Sci. Engng. 40 (2000) 902.
[6] Y. Yang, S. Li, H. Brown, P. Casey, AATCC Rev. 2 (2002) 54.
[7] C.F. Ou, W.C. Li, Y.H. Chen, J. Appl. Polym. Sci. 86 (2002) 1599.
[8] C.F. Ou, J. Polym. Res. 9 (2002) 151.
[9] M. Avrami, J. Chem. Phys. 7 (1939) 1103.
[10] M. Avrami, J. Chem. Phys. 8 (1940) 212.
[11] M. Avrami, J. Chem. Phys. 9 (1941) 177.
[12] B. Wunderlich, Macromolecular Physics, vol. 2, Academic Press, New York, 1976 p. 147.
[13] U.R. Evans, Trans. Faraday Soc. 41 (1945) 365.
[14] T. Ozawa, Polymer 12 (1971) 150.
[15] A. Ziabicki, Appl. Polym. Symp. 6 (1967) 1.
[16] A. Ziabicki, Polymer 12 (1967) 405.
[17] A. Ziabicki, Fundamentals of Fiber Spinning, John Wiley & Sons, New York, 1976 pp. 112–114.
[18] A. Jeziorny, Polymer 19 (1978) 1142.
[19] J.A. Augis, J.E. Bennett, J. Therm. Anal. 13 (1978) 283.
[20] H.E. Kissinger, J. Res. Nat. Bur. Stand. 57 (1956) 217.
[21] R.L. Takhor, Advances in Nucleation and Crystallization of Glasses, American Ceramics Society, Columbus, 1971 pp. 166–172.
[22] S. Vyazovkin, Macromol. Rapid Commun. 23 (2002) 771.

[23] P. Supaphol, J. Appl. Polym. Sci. 78 (2000) 338.
[24] H. Friedman, J. Polym. Sci. C6 (1964-1965) 183.
[25] S. Vyazovkin, J. Comput. Chem. 18 (1997) 393.
[26] S. Vyazovkin, J. Comput. Chem. 22 (2001) 178.
[27] Y.P. Khanna, Polym. Engng. Sci. 30 (1990) 1615.
[28] U. Zhang, H. Zheng, X. Lou, D. Ma, J. Appl. Polym. Sci. 51 (1994) 51.
[29] X.S. Wang, D. Yan, G.H. Tian, X.G. Li, Polym. Engng. Sci. 41 (2001) 1655.